

# Proteomics and Metabolomics Analysis Reveal the Regulation Mechanism of Linoleate Isomerase Activity and Function in *Propionibacterium acnes*

Ying Liu,<sup>§</sup> Yeping Chen,<sup>§</sup> Xiqing Yue, Yingying Liu, Jianting Ning, Libo Li, Junrui Wu, Xue Luo,<sup>\*</sup> and Shuang Zhang<sup>\*</sup>



Cite This: *ACS Omega* 2024, 9, 1643–1655



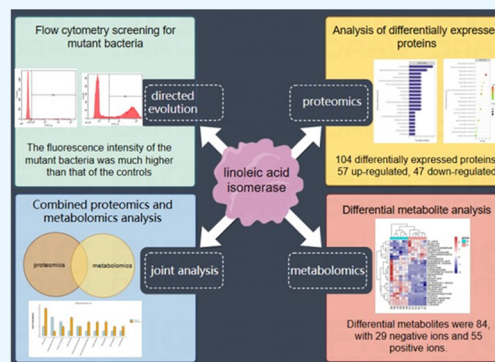
Read Online

ACCESS |

Metrics & More

Article Recommendations

**ABSTRACT:** Conjugated linoleic acid (CLA) holds significant application prospects due to its anticancer, anti-atherosclerosis, lipid-lowering, weight-loss, and growth-promoting functions. The key to its efficient production lies in optimizing the biocatalytic performance of linoleic acid isomerase (LAI). Here, we constructed a *Propionibacterium acnes* mutant library and screened positive mutants with high linoleate isomerase activity. The proteomics and metabolomics were used to explore the mechanism in the regulation of linoleic acid isomerase activity. High-throughput proteomics revealed 104 differentially expressed proteins unique to positive mutant strains of linoleic acid isomerase of which 57 were upregulated and 47 were downregulated. These differentially expressed proteins were primarily involved in galactose metabolism, the phosphotransferase system, starch metabolism, and sucrose metabolism. Differential metabolic pathways were mainly enriched in amino acid biosynthesis, including glutamate metabolism, the Aminoacyl-tRNA biosynthesis pathway, and the ABC transporter pathway. The upregulated metabolites include DL-valine and Acetyl coA, while the downregulated metabolites include Glutamic acid and Phosphoenolpyruvate. Overall, the activity of linoleic acid isomerase in the mutant strain was increased by the regulation of key proteins involved in galactose metabolism, sucrose metabolism, and the phosphotransferase system. This study provides a theoretical basis for the development of high-yield CLA food.



## INTRODUCTION

Conjugated linoleic acid (CLA) refers to a range of octadecadienoic acid isomers that contain conjugated double bonds and are derived from linoleic acid (LA).<sup>1</sup> Of all the CLAs, the cis-9, trans-11 and trans-10, cis-12 isomers are regarded as the primary biological monomers.<sup>2,3</sup> CLA has the effects of inhibiting tumor growth, anti-atherosclerosis, reducing blood lipids, regulating fat metabolism, reducing fat accumulation, promoting growth, etc. and is widely used in medicine, food, and health products.<sup>4–6</sup> Moreover, CLA has broad applications in the cosmetics industry due to its potential benefits for skin health and beauty, including reducing inflammation, improving skin barrier function, and enhancing collagen synthesis.<sup>7,8</sup> CLA can be synthesized through chemical isomerization and microbial LA isomerase (LAI) catalysis. The isomeric composition of CLA produced by isomerization synthesis is complex, posing challenges in isolation and purification. Although the yield of CLA synthesized by LAI is relatively low, the reaction conditions are mild, facilitating easy purification of the product. This method has become a recent research hotspot. Currently, there are mainly two types of LAI derived from microorganisms: a

multienzyme system in lactic acid bacteria with a complex catalytic mechanism and a single enzyme from propionic acid bacteria, with relatively clear catalytic mechanism. Since *Propionibacterium acnes* is a conditional pathogen, LAI is usually heterologously expressed in *Escherichia coli*, yeast, and *Yarrowia lipolytica*.<sup>9</sup> However, the low expression of heterologous LAI has been acknowledged as a limiting factor in its industrial application.<sup>10,11</sup> The LAI of *P. acnes* can catalyze the production of t10, c12 CLA isomers from LA without the involvement of reducing compounds such as NADH or NADPH.<sup>12,13</sup>

In recent years, the low expression of heterologous LAI limits its industrial application, and the optimization of expression is gaining researchers' attention. Directed evolution

**Received:** October 20, 2023  
**Revised:** November 26, 2023  
**Accepted:** November 29, 2023  
**Published:** December 18, 2023



is a widely used technique in biology and interdisciplinary fields, particularly important for improving enzyme expression.<sup>14</sup> This method is effective for detecting and achieving protein modifications and is often considered the first choice for such alterations. The directed evolution process can result in genetic differences between the evolved strain or enzyme and the original one, which may lead to variations in the expression of related proteins or metabolites. In a study on demethylation of coumarins, a library of 7800 mutants was constructed using a combination of site-directed mutagenesis and error-prone PCR. After four rounds of directed evolution and high-throughput screening, the best enzyme was found to be a five-point mutant, which exhibited a positive response to 7-methoxycoumarin. This mutant strain showed a 240-fold increase in demethylation activity of ethoxycoumarin and a 10-fold increase in demethylation activity of 7-methoxycoumarin.<sup>15</sup> Directionally evolved lipase activity was found to be 2-fold higher than the parent,<sup>16</sup> while directionally evolved metalloproteinases showed enhanced tolerance to organic solvents.<sup>17</sup>

In recent years, the rapid development of genomics technology has enabled the comparison and analysis of different aspects of proteins, including their fine structure, translation processes, and modification processes. The bioinformatics-based pairing method can identify microorganisms involved in biosynthesis through non-targeted metabolic analysis of molecular substances present in natural products.<sup>18</sup> Through tracking the process of metabolite changes and detecting the diversity of small molecular substances in cells, it can identify new biosynthetic pathways related to small organisms.<sup>19,20</sup> When investigating the production of differentially expressed proteins of lactic acid during *Bacillus coagulans* fermentation using different carbon sources, it was found that these proteins were mainly involved in pathways such as glycolysis, coenzyme A biosynthesis, pyruvate metabolism, and the tricarboxylic acid cycle (TCA).<sup>21</sup>

In this study, we employed directed evolution technology to obtain *P. acnes* mutant strains with increased LAI activity. First, we constructed a mutant library and screened the positive mutants. We then utilized label-free proteomics technology to analyze the differential protein expression profile and track the changes in protein expression. Non-targeted metabolomics liquid chromatography/mass spectrometry (LC/MS) technology is utilized to analyze differential metabolites, and subsequently, proteomics and metabolomics data are combined to identify proteins and metabolic pathways involved in the mutant strain and control strain at both the protein and metabolite level. Overall, our findings provide insights into the relationship between LAI expression and function.

## MATERIALS AND METHODS

**Strains and Plasmids.** The strain *P. acnes* CICC 10864 was consistently cultured in our laboratory. The pT-lai-p plasmid was previously constructed as described in ref. 9 We constructed two new recombinant plasmids, pCold-lai-p-gfp and pCold-yclai-p-gfp. *E. coli* was cultured in fresh LB liquid medium and incubated at 37 °C and 180 rpm.

**Construction of Mutant Strains and Flow Cytometry Assays.** The LAI gene (lai-p) of plasmid pT-lai-p was utilized as a template to construct the mutant library via error-prone PCR. As a control, the pCold-lai-p-gfp plasmid was transferred into *E. coli*. Mutated bacteria with high expression of LAI were screened using flow cytometry at a concentration of 10<sup>6</sup> cells

per mL. The cells were resuspended and injected into a BD FACS Aria flow cytometer; detection was performed using a 488 nm laser excitation wavelength; and fluorescence measurements were recorded within the 515–545 nm range, using a voltage of 600 V and a photomultiplier tube with logarithmic gain. The positive cells were gated on a fluorescence double plot as specified in each experiment. The P1 gate ensures cell integrity and viability, while at the P2 gate, a break is introduced. It can detect the fluorescence intensity of mutant bacteria, and the intensity of mutant bacteria passing through the P2 gate is relatively high, providing information about the strong lai activity of the mutant bacteria. Collect P2 gate strains, place them in a 96-well plate in a shaking incubator for cultivation at 37 °C, and determine the production of CLA in mutant bacteria.

**Label-Free Proteomic Analysis. Protein Digestion and Liquid Chromatography Tandem Mass Spectrometry (LC-MS/MS) Analysis.** Protein multidigestion was conducted using the filter-aided sample preparation (FASP) method reported by Wiśniewski et al.<sup>22</sup> Briefly, 200 µg of protein was mixed with 30 µL of SDT buffer, and the mixture was washed twice between each ultrafiltration with 100 µL of UA buffer (8 M urea, 150 mM Tris-HCl, pH 8.0), followed by two washes with 100 µL of 25 mM NH<sub>4</sub>HCO<sub>3</sub> buffer. The protein was then digested with 4 µg of trypsin in 40 µL of 25 mM NH<sub>4</sub>HCO<sub>3</sub> at 37 °C overnight. The filtrated peptides were reconstituted in 40 µL of 0.1% formic acid (v/v), and LC-MS/MS analysis was performed by using a Q Exactive mass spectrometer coupled to an EASY-nLC system (Thermo Fisher Scientific). Peptides were loaded onto a nanoViper C18 reversed-phase trap column (Acclaim PepMap100, 100 µm × 2 cm, Thermo Fisher) linked to a C18 reversed-phase analytical column (Easy column, 75 µm × 10 cm, 3 µm resin, Thermo Scientific). Separation employed buffer A (0.1% formic acid) and buffer B (84% acetonitrile and 0.1% formic acid) at 300 nL/min. MS operated in positive ionization mode using a data-dependent top 10 method for higher-energy collisional dissociation (HCD) fragmentation. Automatic gain control (AGC) target was 3e6 with a 10 ms maximum injection time. Dynamic exclusion was set at 40.0 s. Survey and HCD spectra were acquired at resolutions of 70,000 and 17,500 at 200 m/z, respectively. Isolation width: 2 m/z. Normalized collision energy was 30 eV; underfill ratio was 0.1%, and peptide recognition mode was enabled.

**Protein Identification and Kyoto Encyclopedia of Genes and Genomes (KEGG) Pathway Annotation Analysis.** The MS data were analyzed using MaxQuant software (version 1.5.3.17). To search for KEGG Orthologies and map them to pathways in KEGG, the DEP FASTA protein sequence was compared with the online KEGG database (Release 98.1) available at <http://geneontology.org/>.

**Untargeted Metabolomics. Sample Extraction.** The sample was slowly thawed at 4 °C and added with a precooled methanol/acetonitrile/H<sub>2</sub>O solution (2:2:1, v/v). Subsequently, the mixture was subjected to low-temperature ultrasonication and vortexing to precipitate proteins. The samples were then maintained at –20 °C for 1 h, followed by the collection of the supernatant through centrifugation at 4 °C and 14,000g for 20 min. The supernatants were removed, and the samples were dried under a vacuum. Next, the sample was added with 100 µL of aqueous acetonitrile solution (acetonitrile/H<sub>2</sub>O = 1:1, v/v) and analyzed using MS.

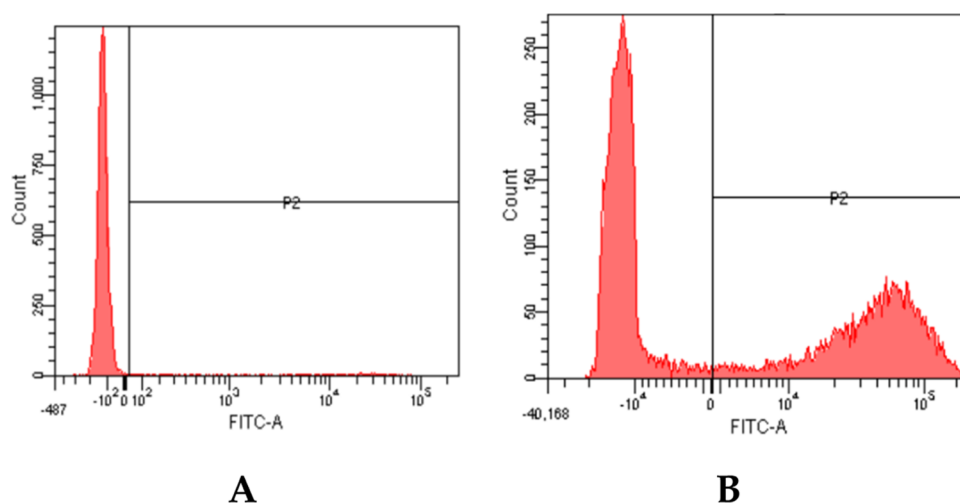


**Figure 1.** Flow cytometry sorting. (A) Sorting of the control group. (B) Sorting of experimental groups.

**Table 1.** Absorbance of Mutant Bacteria

no.	absorption value						
84	0.8649 ± 0.0007s	123	0.9016 ± 0.0008e	173	0.9364 ± 0.0009n	229	1.2979 ± 0.0007a
87	1.1014 ± 0.0008c	132	1.0370 ± 0.0005g	188	0.9470 ± 0.0005m	234	0.9549 ± 0.0008j
90	0.8656 ± 0.0007r	137	0.8538 ± 0.0002s	191	1.2936 ± 0.0007b	238	0.9489 ± 0.0001k
96	0.8465 ± 0.0006t	141	0.8759 ± 0.0001q	197	1.0706 ± 0.0014e	ck	0.2541 ± 0.0002v
101	1.0084 ± 0.0006h	146	0.9312 ± 0.0004o	206	0.9971 ± 0.0005h		
105	1.0636 ± 0.0005f	149	0.9474 ± 0.0008l	213	1.0681 ± 0.0006d		
116	0.8456 ± 0.0009u	159	0.9074 ± 0.0010p	215	1.0051 ± 0.0005i		

**Chromatography-MS Analysis.** Two  $\mu\text{L}$  portion of the sample was loaded onto an Agilent 1290 Infinity LC Ultra High-Performance Liquid Chromatography HILIC column at a flow rate of 0.5 mL/min. Primary and secondary spectra of the samples were collected using an AB Triple TOF 6600 mass spectrometer. The phase A is ammonium acetate/ammonia/ $\text{H}_2\text{O}$  solution (25 mM  $\text{CH}_3\text{COONH}_4$ , 25 mM  $\text{NH}_3\cdot\text{H}_2\text{O}$ ), and the phase B is acetonitrile. The gradient elution conditions are 0–7 min: 95% of phase B; 7–8 min: 65% of phase B; 8–9.1 min: 40% of phase B; 9.1–12 min: 95% of phase B.

**Combined Proteomic and Metabolomic Analyses.** Differential expression profiles of peptides under different conditions were analyzed for significantly enriched pathways from the KEGG database. Quantitative data was Z-score normalized, and a heatmap was generated using R version 3.5.1. Euclidean distance matrix computation and complete linkage hierarchical clustering were used for heatmap.

**Database Search.** InterProScan software (<http://www.ebi.ac.uk/interpro/>) was used to annotate the Gene Ontology (GO) functions based on protein sequence alignment. We also annotated KEGG pathways using [http://www.genome.jp/kaas-bin/kaas\\_main](http://www.genome.jp/kaas-bin/kaas_main).<sup>23</sup> All experiments were conducted in triplicate, and the data are presented as means  $\pm$  standard deviations.

## RESULTS

**Screening for High-Yielding CLA Mutant Strains.** The control group for this experiment consisted of recombinant bacteria that did not undergo error-prone PCR. Strains crossing gate P1 were all mutant strains with a relatively strong fluorescence intensity. The flow cytometry sorting results are shown in Figure 1. In Figure 1A, depicting the

sorting results for the nonmutant strain pCold-gfp-lai-p, mutant bacteria at gate P2 constituted 2.5% of those at gate P1. Figure 1B illustrates the sorting results for the mutant strain pCold-gfp-yclai-p, yielding a total of 11,913 mutant strains. The selected strains comprised 35.2% of all strains, with 4195 mutant strains exhibiting fluorescence intensity higher than the control group. The screened mutant strains were then subjected to shaking cultivation in a 96-well plate, resulting in 238 mutant strains exhibiting normal growth. The CLA yield of the control bacteria was  $3.3935 \pm 0.0003 \mu\text{g/mL}$ . Among the mutant bacteria, 211 strains (88.7% of all strains) gave higher CLA yield than the control bacteria. Notably, 24 mutant strains exhibited a substantial increase in CLA production, and these strains are listed in Table 1, the highest CLA production (named as P229), corresponding to an absorbance value of  $1.2979 \pm 0.0007$  and a CLA production of  $17.4609 \pm 0.0007 \mu\text{g/mL}$ .

**LC-MS/MS Proteome Identification and Screening of Differentially Expressed Proteins (DEPs).** From high-throughput proteomic analysis, a total of 349,823 secondary spectra were obtained, with 83,174 spectra found to be matched. In total, 16,623 peptide sequences were quantified, of which 15,950 were identified as specific peptides. Among these, 2146 proteins were quantified, with a total of 2110 proteins available for quantitative analysis (Figure 2). The abundance of acquired specific peptides and proteins is substantial, ensuring the reliability of identification and quantification results.

To analyze the differentially expressed proteins between different groups, experimental data were further screened for differences. Proteins were accepted as differentially expressed proteins between the mutagenic bacteria and primitive bacteria groups when the upregulated fold-change values were more

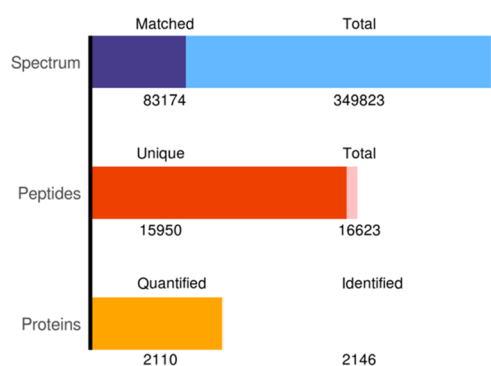


**Figure 2.** Statistical histogram of the identification and quantitative results.

than 2, or the downregulated fold-change values were less than 0.5, and  $p$ -values were less than 0.05.<sup>24</sup> The proteomic analysis revealed a total of 104 differentially expressed proteins, comprising 47 downregulated and 57 upregulated proteins. Among these, there are 20 key differentially expressed proteins, with 6 showing downregulation and 14 exhibiting upregulation (Table 2). Upregulated proteins include arginine ABC transporter permease protein ArtM (artM), D-erythrose-4-phosphate dehydrogenase (epd), PTS system trehalose-specific EIIBC component (treB), PTS system glucose-specific EIIA component (crr), NADP-specific glutamate dehydrogenase (gdhA), ATP-dependent 6-phosphofructokinase isozyme 2 (pfkB), tryptophan-specific transport protein (mtr), and molybdopterin-synthase adenyltransferase (moeB). Downregulated proteins include L-fucose isomerase (fucI) and the PTS system galactitol-specific EIIA component (gatA).

Differentially expressed proteins in the metabolism of hydroxy organic compounds include glpE, ugpQ, epd, and hpaG. MalP is identified as a differentially expressed protein in the metabolism of  $\alpha$ -glucan. In the breakdown process of  $\alpha$ -glucan, malP is also differentially expressed, while fucI is identified as a differentially expressed protein in the metabolism of hexose.

**Identify Proteins for Functional Annotation and Bioinformatics Analysis.** GO analysis was employed to assess the enrichment of specific functions, aiming to identify proteins displaying differential abundance between the control and mutant groups. Figure 3A illustrates the GO annotations of the identified proteins, categorized based on cellular components (CC), molecular functions (MF), and biological processes (BP). The analysis revealed that differentially identified proteins were further classified into 20 hierarchical GO categories, including 3 in CC, 6 in MF, and 11 in BP. In the determination of CC, intrinsic components of the membrane, structural components of the membrane, and membrane parts were significantly enriched in the mutant strains. In the MF assessment, prominent functionalities included enzymatic activities, such as ethanol dehydrogenase activity. In the examination of BP, many proteins were involved in processes such as polyol metabolism, alcohol metabolism, and polyol metabolic processes. The GO classification indicated that differential proteins were primarily concentrated in BP, including the metabolic processes of hydroxy organic compounds,  $\alpha$ -glucan catabolic processes, and hexose catabolic processes.

A volcano plot showing the differentially expressed proteins in the mutant and control groups (Figure 3B) revealed that the majority of upregulated proteins were associated with  $\alpha$ -glucan and organic hydroxyl compound metabolism, while most downregulated proteins were related to hexose metabolism.

The 179 differentially expressed proteins identified in the study were classified into five intracellular categories (Figure 3C). The majority of differentially expressed proteins were located in the cytoplasm, totaling 114, representing 64% of the total, followed by 30 proteins in the intracellular membrane, accounting for 17%; 27 proteins in the periplasm, constituting 15%; 5 differentially expressed proteins were found in the extracellular space, and the least number of differentially expressed proteins, 3, were located in the outer membrane.

**Enrichment Analysis of Differentially Expressed Proteins.** A total of 170 proteins were systematically

**Table 2.** Key Differentially Expressed Proteins Information

regulated type	name	protein description	fold-change	p-value
downregulated proteins	gatA	PTS system galactitol-specific EIIA component	0.374	0.012
	tgt	queuine tRNA-ribosyltransferase	0.497	0.036
	nuoE	NADH-quinone oxidoreductase subunit E	0.495	0.034
	fucI	L-fucose isomerase	0.209	0.001
	ycbB	probable L,D-transpeptidase YcbB	0.489	0.026
	hemG	protoporphyrinogen IX dehydrogenase	0.482	0.026
	gdhA	NADP-specific glutamate dehydrogenase	2.063	0.002
upregulated proteins	treB	PTS system trehalose-specific EIIBC component	2.033	0.025
	crr	PTS system glucose-specific EIIA component	2.125	0.015
	glpE	thiosulfate sulfur transferase GlpE	2.402	0.004
	epd	D-erythrose-4-phosphate dehydrogenase	5.297	0.009
	malP	maltodextrin phosphorylase	2.238	0.008
	pfkB	ATP-dependent 6-phosphofructokinase isozyme 2	2.333	0.003
	mtr	tryptophan-specific transport protein	3.193	0.003
	artM	arginine ABC transporter permease protein ArtM	5.956	0.001
	abgA	p-aminobenzoyl-glutamate hydrolase subunit A	4.924	0.048
	glcD	glycolate oxidase subunit GlcD	6.021	0.003
	mdtE	multidrug resistance protein MdtE	5.375	0.021
	cspA	cold shock protein CspA	3.950	0.012
	moeB	molybdopterin-synthase adenyltransferase	2.693	0.001

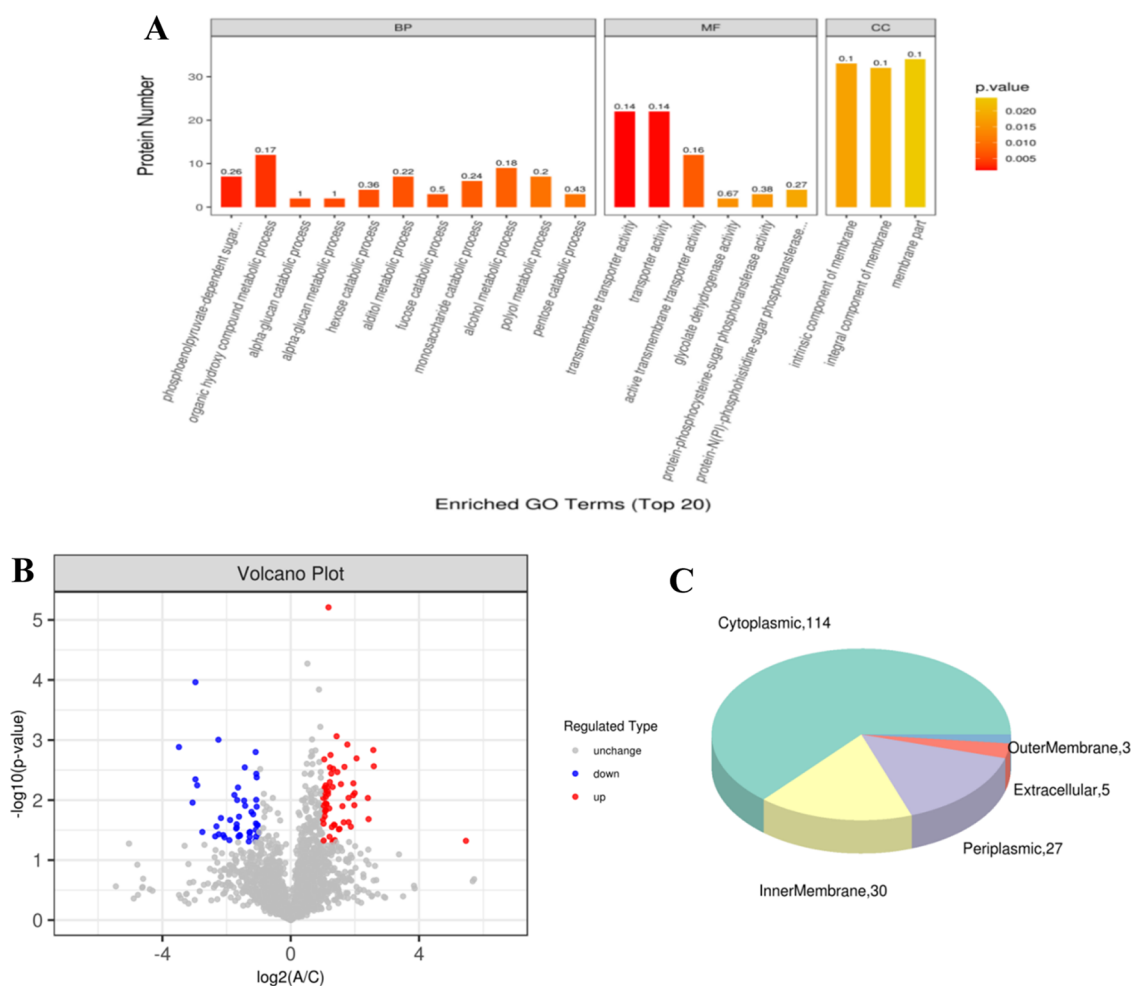


**Figure 3.** Identify proteins for functional annotation and bioinformatics analysis. (A) Gene ontology classification of proteins between infected and control groups, including biological processes (BP), molecular functions (MF), and cellular components (CC). (B) The volcano plot shows up- (red) or downregulated (blue) proteins between mutated and control groups. (C) Differentially expressed protein subcellular location pie chart.

categorized into 12 KEGG categories. Out of these, 104 distinct proteins demonstrated statistically significant differences in molecular functions ( $p < 0.05$ ) spanning diverse biological processes and cellular locations. The findings depicted in Figure 4(A) highlight the correlation between the functions of these 104 differentially abundant proteins (DAPs) and the functional domains (N-terminal and C-terminal domains) associated with the FGGY carbohydrate kinase family. Employing KEGG analysis, we explored pathways enriched with DAPs, identifying associations with 11 signaling pathways. Figure 4(B) illustrates that the differentially expressed proteins predominantly cluster in galactose metabolism, phosphotransferase systems, and starch and sucrose metabolism. Specifically, two DAPs, pfkB and gatA, were implicated in the galactose metabolism pathway, while treB, gatA, and crr were linked to the phosphotransferase system. Additionally, malP and treB were associated with starch and sucrose metabolism. In light of this analysis, we posit that the heightened activity of linoleic acid isomerase in the mutant bacteria instigated alterations in the expression levels of pfkB, treB, and gatA.

**Screening and Cluster Analysis of Differential Metabolites.** We performed a non-targeted metabolomic analysis to identify differential metabolites and metabolic pathways influencing LAI activity. The criteria for screening

differential metabolites were set as Fold-change  $\geq 1.2$  or  $\leq 0.83$  with a  $p$ -value  $< 0.05$ . To visually represent the changes in differential metabolites of the mutated strain's linoleic acid isomerase more intuitively, all screened differential metabolites in both positive (POS) and negative (NEG) ion modes were subjected to cluster analysis (Figure 5A,B). A total of 55 metabolites were detected in positive ion mode, while 29 metabolites were detected in negative ion mode (Figure 5C,D).

**Enrichment Analysis of Differential Metabolites.** As shown in Figure 6, the metabolic pathways associated with differentially expressed metabolites using the KEGG database showed a significant enrichment of amino acids, including L-citrulline, aspartic acid, glutamic acid, phenylalanine, and valine. Notably, many of the initial metabolites in the purine metabolic pathway originate from various amino acid metabolic pathways, and sugar metabolism is closely linked to amino acid synthesis. It is worth mentioning that amino acid site mutations in *P. acnes* can affect the LAI activity. This finding suggests that the increase in activity may be due to amino acid mutations that affect amino acid metabolism.

Based on the results of metabolomics, 15 major metabolic pathways related to such metabolites were organized (Table 3). The results indicate that after mutation of the linoleic acid isomerase, differential metabolites primarily enriched in

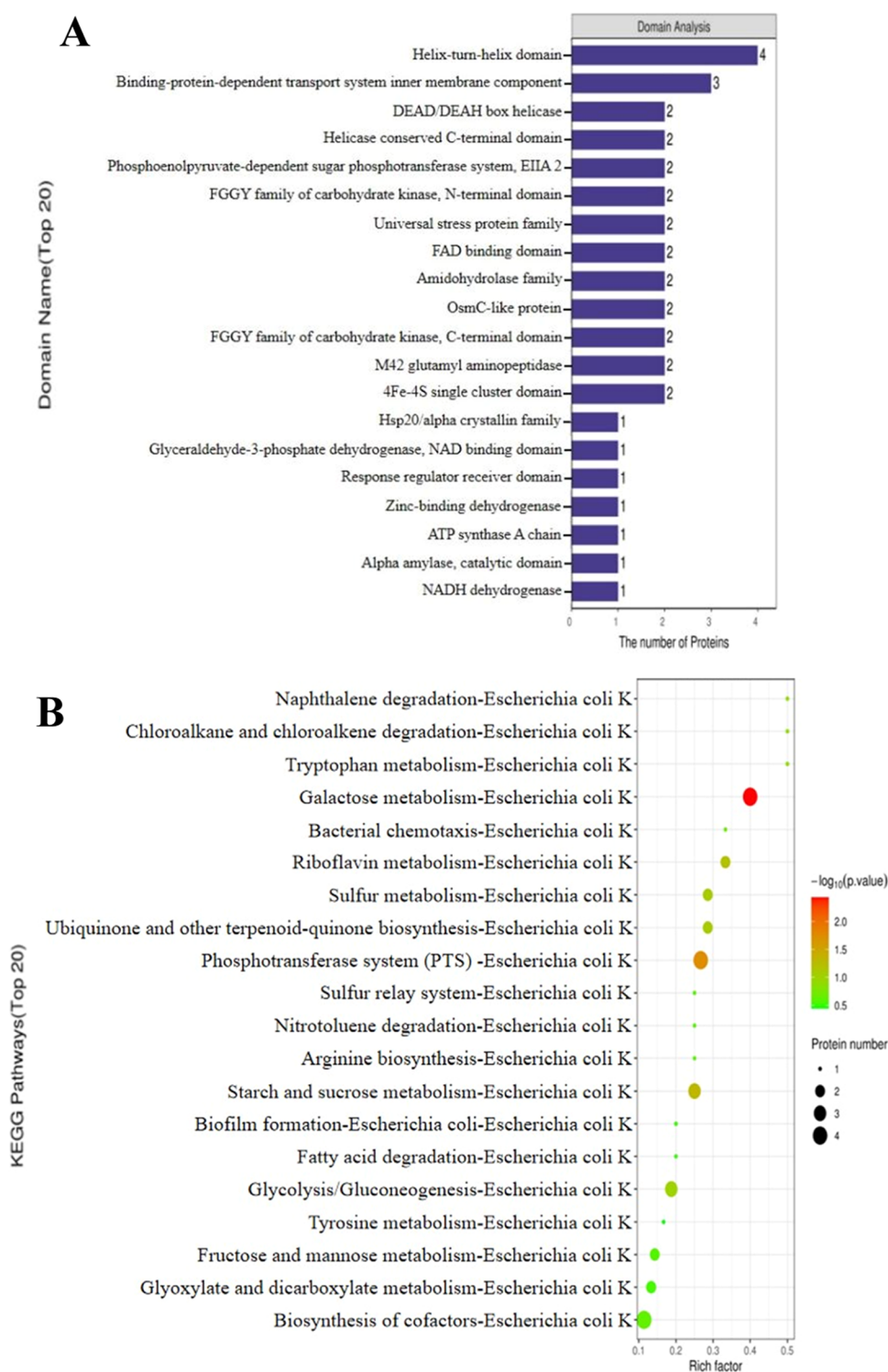


**Figure 4.** Enrichment analysis of differentially abundant proteins. (A) Enrichment analysis of protein domains. (B) KEGG pathway enrichment analysis. The size and color of each bubble represent the number of proteins enriched in the pathway and the enrichment significance, respectively.

biosynthesis of amino acids, carbon metabolism, ABC transporters, arginine biosynthesis, aminoacyl-tRNA biosynthesis, glutathione metabolism, histidine metabolism, alanine, aspartate and glutamate metabolism, taurine, and hypotaurine metabolism, with a small fraction of differential metabolites enriching in the citrate cycle (TCA) and glycolysis, among other metabolic pathways.

#### Metabolic Pathway Map of Differential Metabolites.

The main metabolic pathways enriched with differential metabolites were mapped to the metabolite change network. As shown in Figure 7(A) for the TCA cycle metabolic pathway, Map ID: eco00020, URL:[https://www.kegg.jp/kegg-bin/show\\_pathway?eco00020+C00074](https://www.kegg.jp/kegg-bin/show_pathway?eco00020+C00074). As shown in Figure 7(B) for aspartate, glutamate, and alanine metabolic pathways,

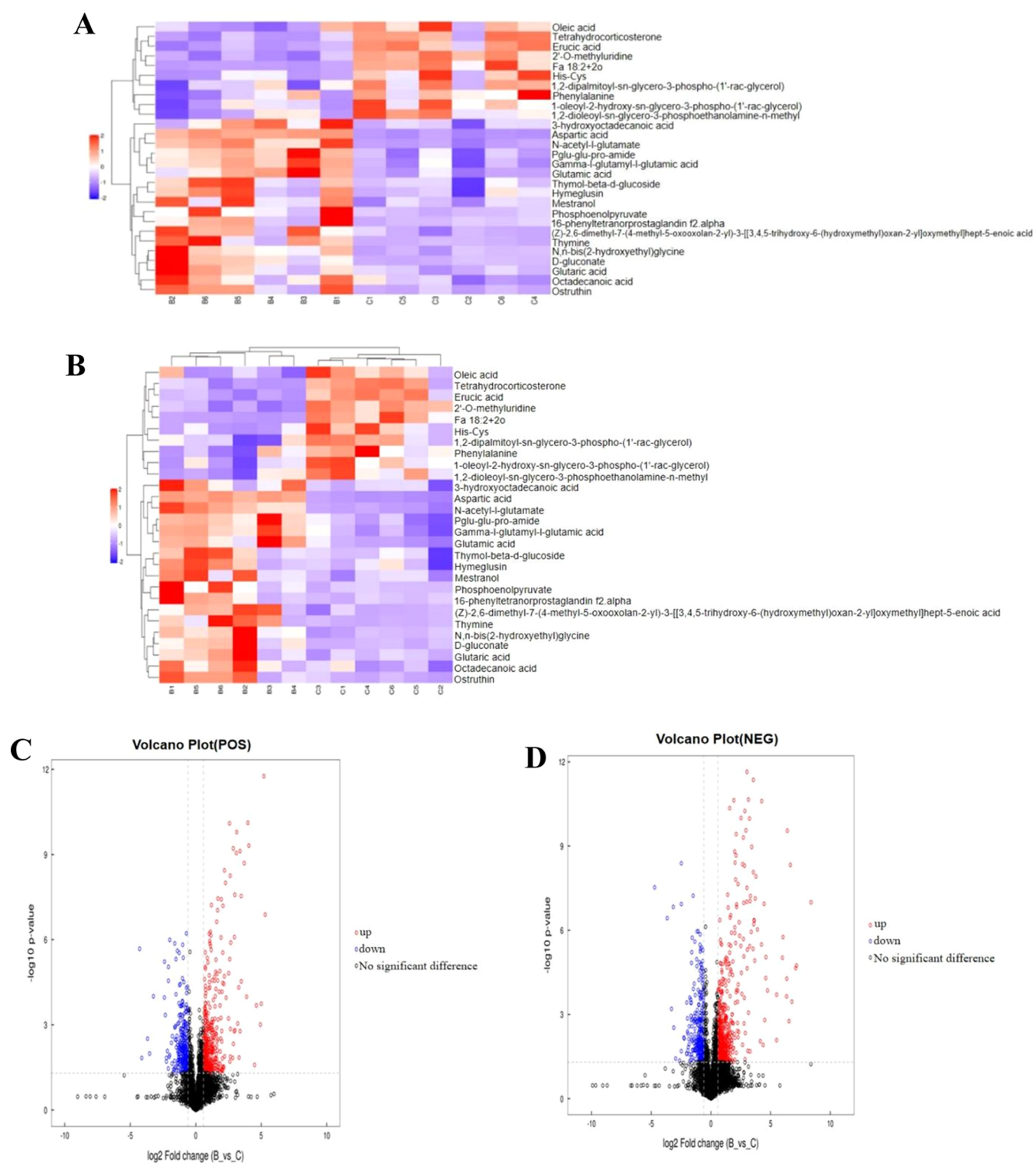


**Figure 5.** Volcano map of differential metabolites and differential metabolite cluster analysis. (A) Control group. (B) Experimental group. (C) Volcano-pos. (D) Volcano-neg.

Map ID: eco00250, URL:[https://www.kegg.jp/kegg-bin/show\\_pathway?eco00250+C00025](https://www.kegg.jp/kegg-bin/show_pathway?eco00250+C00025).

The metabolic pathway map can intuitively display the changes in metabolites in mutant bacteria. The metabolites enriched in the TCA cycle pathway include acetyl CoA and phosphoenolpyruvic acid. The main metabolites in the metabolic pathways of alanine, aspartic acid, and glutamic acid include DL-glutamic acid and L-aspartic acid. The red circle

represents upregulated differential metabolites, and the green square represents upregulated differential metabolites.

**KEGG Pathway Annotation Analysis.** The differentially expressed proteins and metabolites identified were annotated by using KEGG pathway analysis. Figure 8 illustrates the annotation results of the differentially expressed proteins and metabolites. Specifically, four differentially expressed proteins were annotated to phosphate in the pentose pathway; three

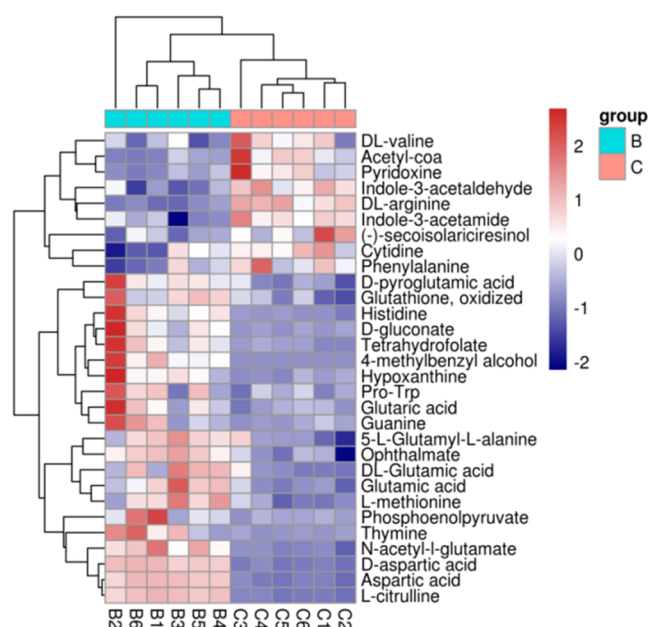


**Figure 6.** Differential metabolite clustering heatmap of the KEGG pathway.

differentially expressed proteins were enriched in the glycolysis/gluconeogenesis pathway; and the remaining annotated proteins were involved in ABC transporters, glyoxylate and dicarboxylate metabolism, arginine biosynthesis, alanine, aspartate, and glutamate metabolism, tryptophan metabolism, methane metabolism, fatty acid degradation, and pyruvate metabolism. Moreover, six differentially expressed metabolites were enriched in the ABC transporter category, four differentially expressed metabolites were annotated to arginine biosynthesis, and the remaining annotated metabolites were involved in glyoxylic acid and dicarboxylic acid metabolism, alanine, aspartate, and glutamate metabolism, tryptophan metabolism, methane metabolism, fatty acid degradation, and pyruvate metabolism.

## DISCUSSION

**GO Classification of Proteins.** Through GO classification, we found that the proteins showing differential expression were predominantly associated with biological processes such as the phosphoenolpyruvate-dependent sugar phosphotransferase system, metabolic processes related to organic hydroxyl compounds,  $\alpha$ -glucan metabolism, glycan decomposition, and hexose catabolism. The uptake and metabolism of sucrose by *Clostridium butyricum* ZJU 8235 provided conclusive evidence of a phosphotransferase system (PTS) that is dependent on phenol pyruvate activity in bacteria responsible for producing butyric acid. This discovery marks a significant contribution to the field.<sup>25</sup> The mycobacterial capsules, which constitute the outermost layer of the mycobacterial cell envelope, play a crucial role in regulating the immune response of the host and influencing the toxicity of mycobacterial bacteria. These findings shed light on the significance of mycobacterial capsules in understanding the pathogenesis of mycobacterial infections.<sup>26</sup>

In this study, we identified several differentially expressed proteins involved in the phosphoenolpyruvate-dependent sugar phosphotransferase system, including treB (the specific EIIBC component of the trehalose PTS), gatA (the specific EIIA component of the galactose PTS), and crr (the glucose-specific component of the EIIA PTS). Furthermore, we found differentially expressed proteins in the metabolism of organic hydroxyl compounds, such as glpE (a thiosulfate sulfur transferase), ugpQ (a cytoplasmic glycerophosphodiester phosphodiesterase), d-erythrose-4-phosphate dehydrogenase, and 4-hydroxyphenyl acetate degradation bifunctional isomerase/decarboxylase. Our analysis also revealed differentially expressed proteins involved in the metabolism of  $\alpha$ -glucan, such as maltodextrin phosphorylase (malP), and in hexose catabolism, such as l-fucose isomerase.

Furthermore, we observed several differential functions, including transmembrane transporter activity, transport activity, active transmembrane transporter activity, glycolate dehydrogenase activity, and protein phosphocysteine sugar phosphotransferase activity. In addition, we found various differential cellular components such as the inherent components of the membrane, overall composition of the

**Table 3. Differential Metabolic Pathway Information**

ID	name	enriched differential metabolites <sup>a</sup>	numbers
eco01230	biosynthesis of amino acids	aspartic acid, N-acetyl-L-glutamate, glutamic acid, phenylalanine, DL-valine <sup>b</sup>	5
eco01200	carbon metabolism	aspartic acid, D-gluconate, phosphoenolpyruvate, acetyl-coA, tetrahydrofolate	5
eco02010	ABC transporter	aspartic acid, phenylalanine, histidine, DL-valine, glutamic acid	5
eco00220	arginine biosynthesis	aspartic acid, N-acetyl-L-glutamate, glutamic acid, L-citrulline	4
eco00970	aminoacyl-tRNA biosynthesis	aspartic acid, DL-glutamic acid, phenylalanine, L-methionine	4
eco00480	glutathione metabolism	glutamic acid, acetyl-coA, oxidized glutathione, DL-glutamic acid	4
eco00340	histidine metabolism	aspartic acid, DL-glutamic acid, histidine, glutamic acid	4
eco00250	alanine, aspartate and glutamate metabolism	glutamic acid, D-aspartic acid, DL-glutamic acid	3
eco00430	taurine and hypotaurine metabolism	glutamic acid, acetyl-coA, DL-glutamic acid	3
eco00020	citrate cycle (TCA cycle)	phosphoenolpyruvate, acetyl-coA	2
eco00290	valine, leucine and isoleucine biosynthesis	acetyl-coA, DL-valine	2
eco00770	pantothenate and CoA biosynthesis	aspartic acid, DL-valine	2
eco00620	pyruvate metabolism	phosphoenolpyruvate, acetyl-coA	2
eco00010	glycolysis/gluconeogenesis	phosphoenolpyruvate, acetyl-coA	2
eco02060	phosphotransferase system	phosphoenolpyruvate	1

<sup>a</sup>All amino acids referred to in the table are L-amino acids unless otherwise noted. <sup>b</sup>DL-amino acids contain both L- and D-amino acids and are also known as racemic mixtures.

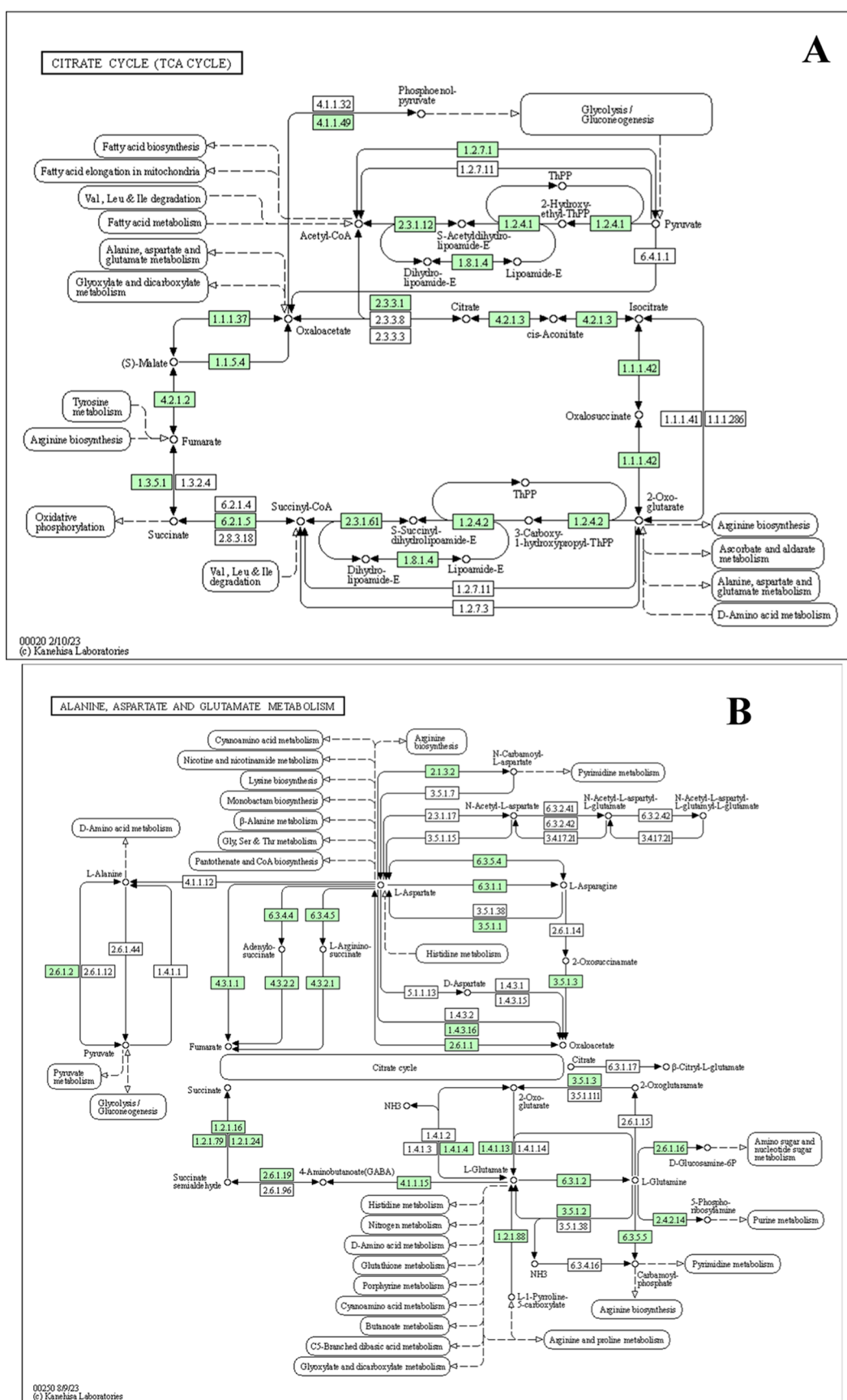


**Figure 7.** Metabolic pathway map of differential metabolites. (A) TCA cycle metabolic pathway. (B) Alanine, aspartate, and glutamate metabolic pathways.

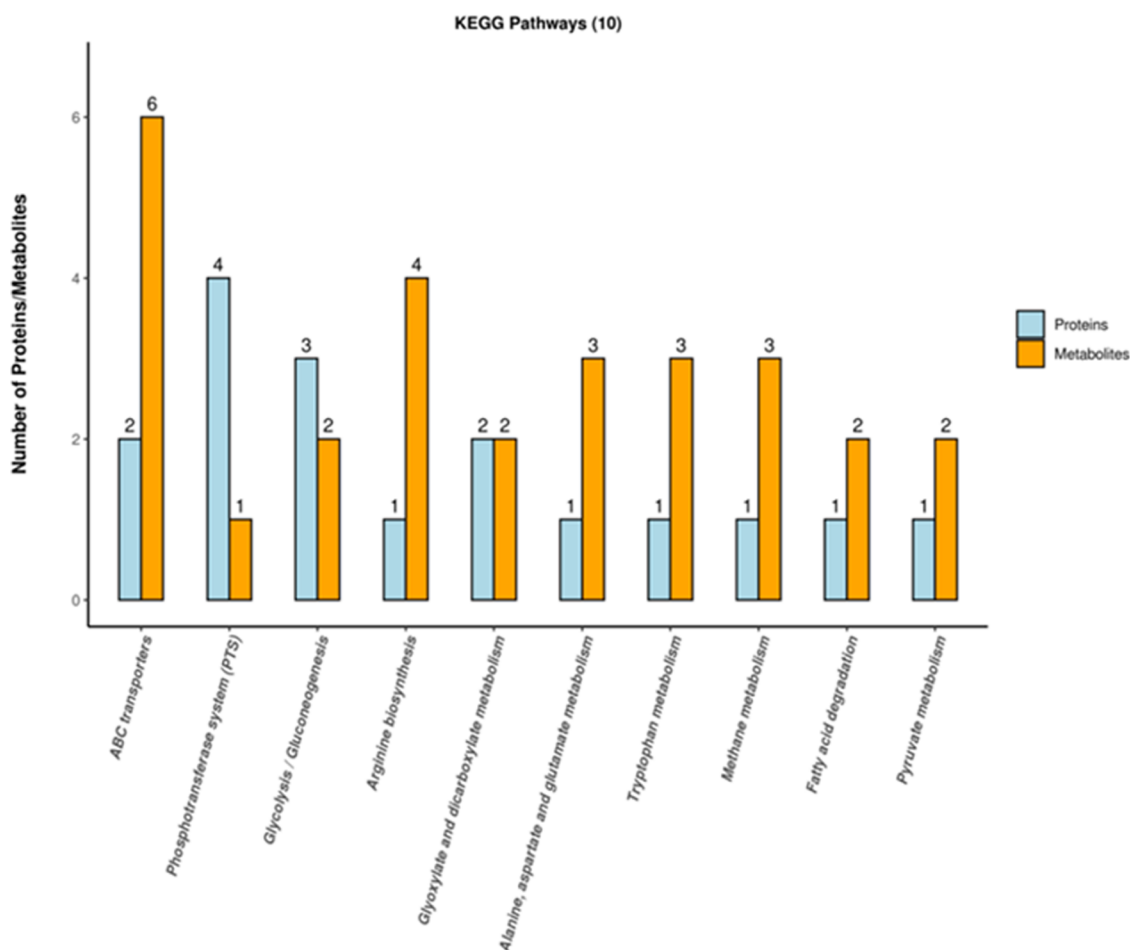


Figure 8. KEGG pathway notes.

membrane, and membrane parts. These findings provide a comprehensive understanding of the molecular mechanisms underlying the observed biological processes.

**Metabolic Pathways of Differentially Expressed Proteins.** Our enrichment analysis of metabolic pathways revealed that the differentially expressed proteins were predominantly enriched in galactose metabolism, the phosphotransferase system (PTS), and the metabolism of starch and sucrose. Within the galactose metabolism pathway, we identified two differentially expressed proteins, namely, ATP-dependent 6-phosphofructokinase isoenzyme 2 and *gatA* (the specific EIIC component of galactose in the PTS). Similarly, we found that four differentially expressed proteins, *treB* (the specific EIIBC component of the trehalose PTS) and *gatA*, were associated with the PTS, while *malP* and *treB* were involved in the metabolism of starch and sucrose. Based on our analysis, we hypothesize that the increased enzyme activity of recombinant bacteria linoleate isomerase alters the expression of *treB*, *gatA*, and *malP*, leading to changes in galactose metabolism and the PTS, starch, and sucrose metabolism. Hemmi's successfully isolating the gene responsible for encoding the *E. coli* PTS demonstrated that this gene played a crucial role in increasing the incorporation of 1-DX into bacterial cells.<sup>27</sup> These findings highlight the importance of PTS in bacterial metabolism and its potential for biotechnological applications.

**Differentially Expressed Proteins.** Bacteria use three types of transporters to uptake sugars and sugar alcohols. The

first type is PTS, which was discussed earlier. The second type is the secondary carrier, driven by  $H^+$ ,  $Na^+$ , or other gradients on the plasma membrane, facilitating unidirectional transport, reverse transport, or codirectional coordination of solutes. The third type is ABC transporters.<sup>28</sup> In *P. acnes*, the metabolic regulation of amino acids is crucial for maintaining growth, particularly in later stages.<sup>29</sup> In this study, we observed upregulation of some proteins related to transport and amino acid metabolism. For instance, NADP-specific glutamate dehydrogenase, which is involved in glutamate metabolism, was differentially expressed. Additionally, upregulation of a tryptophan-specific transport protein may facilitate the uptake of dipeptides and oligopeptides from the growth environment. We found the arginine ABC transporter permease protein *artM* to be upregulated, indicating an increased amino acid uptake. Glutamate reductase (GPR), which catalyzes the NADPH-dependent reduction of L-glutamyl 5-phosphate to L-glutamic acid 5-semialdehyde and phosphate,<sup>30</sup> was also upregulated. Notably, GPR is expressed on the cell surface of many bacterial species.<sup>31</sup> In *E. coli*, GPR has a low ability to reduce N-acetyl glutamyl phosphate.<sup>32</sup>

Deayton et al. investigated the differential protein expression profiles of evolved strains of *Lactobacillus brevis* under nutritional stress using proteomics technology and found 36 differentially expressed proteins after 75 days compared to the original strains. These proteins were primarily associated with glucose metabolism, glycerolipid metabolism, and amino acid metabolism.<sup>33</sup> Bove's study on differentially expressed proteins

in *Lactobacillus rhamnosus* in ordinary MRS medium and simulated cheese maturation environment revealed that 59 proteins were significantly upregulated and 62 proteins were significantly downregulated in cheese medium. These proteins were found to be related to amino acid, carbohydrate, nucleic acid, and citric acid metabolism; protein synthesis and hydrolysis; extracellular polysaccharide synthesis; and stress responses.<sup>34</sup> The previous results are consistent with our current findings, indicating significant alterations in several metabolism-related proteins.

Purine nucleotides play a crucial role in the synthesis of macromolecules such as DNA and RNA and are essential for the growth of lactic acid bacteria.<sup>35</sup> Our data suggested upregulation of proteins involved in the purine biosynthesis pathway such as molybdopterin-synthase adenylyltransferase. Additionally, the DNA polymerase III subunit tau and guanylate kinase, which are associated with purine metabolism, were differentially expressed. DNA polymerase participates in DNA replication, recombination, and repair, and its tau subunit catalyzes the directional extension of the DNA template at the 3' end of the DNA chain.<sup>36</sup> Guanylate kinase is a monomeric protein that transfers a phosphate group from adenosine triphosphate to GMP in the presence of Mg<sup>2+</sup>.<sup>37</sup> This protein is required for the conversion of GMP to GDP in guanosine triphosphate synthesis<sup>38</sup> and also activates antiviral drugs such as acyclovir and ganciclovir.<sup>39</sup> Similar to adenylate kinase, guanylate kinase has a glycine-rich region near the N-terminus that forms a large anion pore to accept the phosphate of ATP.<sup>40</sup>

## CONCLUSIONS

The application prospects of CLA are extremely broad. To enhance CLA production, we obtained an enzyme with increased activity, LAI, through mutation. Subsequently, we conducted an in-depth exploration of the mechanisms underlying the enhanced activity of LAI through proteomics and metabolomics. Interestingly, our research indicates that *treB* and *gatA* participate in various metabolic pathways and are associated with sugar metabolism. The upregulation of *gdhA* expression is conducive to promoting the conversion of LA to CLA, and the upregulation of acetyl-CoA expression is also beneficial for the accumulation of unsaturated fatty acids. In summary, analysis of the CLA synthesis pathway in genetically engineered strains reveals that upregulating key proteins in carbohydrate and glutamate metabolism can increase CLA production. This anticipated improvement in the enzymatic performance is expected to contribute to a more streamlined and cost-effective production process, ultimately promoting the development of high-yield CLA foods.

## AUTHOR INFORMATION

### Corresponding Authors

**Xue Luo** – College of Food Science, Shenyang Agricultural University, Shenyang 110000, China; [orcid.org/0000-0002-3549-2936](https://orcid.org/0000-0002-3549-2936); Email: [luoxue@syau.edu.cn](mailto:luoxue@syau.edu.cn)

**Shuang Zhang** – College of Food Science, Northeast Agricultural University, Harbin 150000, China; Email: [szhang@neau.edu.cn](mailto:szhang@neau.edu.cn)

### Authors

**Ying Liu** – College of Food Science, Shenyang Agricultural University, Shenyang 110000, China

**Yeping Chen** – College of Food Science, Shenyang Agricultural University, Shenyang 110000, China; [orcid.org/0009-0007-5067-8740](https://orcid.org/0009-0007-5067-8740)

**Xiqing Yue** – College of Food Science, Shenyang Agricultural University, Shenyang 110000, China; [orcid.org/0000-0001-5558-1461](https://orcid.org/0000-0001-5558-1461)

**Yingying Liu** – College of Food Science, Shenyang Agricultural University, Shenyang 110000, China

**Jianting Ning** – College of Food Science, Shenyang Agricultural University, Shenyang 110000, China; [orcid.org/0000-0002-4030-9710](https://orcid.org/0000-0002-4030-9710)

**Libo Li** – College of Food Science, Shenyang Agricultural University, Shenyang 110000, China

**Junrui Wu** – College of Food Science, Shenyang Agricultural University, Shenyang 110000, China

Complete contact information is available at:

<https://pubs.acs.org/10.1021/acsomega.3c08243>

## Author Contributions

<sup>§</sup>C.Y. and L.Y. contributed equally to this work. X.L. and S.Z. contributed to conceptualization; Y.L. contributed to methodology; Y.C. contributed to software; Y.L., J.N., and L.L. contributed to validation; X.Y. contributed to resources; Y.L. contributed to writing—original draft preparation; X.L. and S.Z. contributed to writing—review and editing; J.W. contributed to project administration. All authors have read and agreed to the published version of the manuscript.

## Funding

This work was supported by the Scientific Research Project of Liaoning Provincial Department of Education (LJKMZ20221036), National Natural Science Foundation of China (Grant No. 31701623).

## Notes

The authors declare no competing financial interest.

## ACKNOWLEDGMENTS

The authors thank College of Food Science, Shenyang Agricultural University of Shenyang City for their assistance during this project.

## ABBREVIATIONS

CLA, conjugated linoleic acid; LA, linoleic acid; LAI, linoleic acid isomerase of *P. acnes* origin; LC-MS/MS, liquid chromatography tandem mass spectrometry; KEGG, kyoto encyclopedia of genes and genomes; GO, gene ontology; TCA, trichloroacetic acid; PTS, phosphotransferase system

## REFERENCES

- Shenderov, B. A.; Sinita, A. V.; Zakharchenko, M. M.; Lang, C. *Metabiotics: Present State*. In *Challenges and Perspectives*, 1st ed.; Springer Nature: Cham, Switzerland, 2020; pp 5–9.
- Dahiya, D. K.; Puniya, A. K. Optimisation of fermentation variables for conjugated linoleic acid bioconversion by *Lactobacillus fermentum* DDHI 27 in modified skim milk. *Int. J. Dairy Technol.* **2018**, *71*, 46–55.
- Tapia, A. M.; Bautista, J. A. N.; Mendoza, B. C.; Pham, L. J.; Sarmago, I. G.; Oliveros, M. C. R. Production of conjugated linoleic acid by lactic acid bacteria: Screening and optimization. *Philipp. J. Sci.* **2019**, *148*, 457–464.
- Baliyan, N.; Maurya, A.; Kumar, A.; Agnihotri, V. K.; Kumar, R. Probiotics from the bovine raw milk of Lahaul valley showed cis-9, trans-11 conjugated linoleic acid isomer and antioxidant activity with

food formulation ability. *LWT* **2023**, *176*, No. 114553, DOI: 10.1016/j.lwt.2023.114553.

(5) Ayivi, R. D.; Gyawali, R.; Krastanov, A.; Aljaloud, S. O.; Worku, M.; Tahergorabi, R.; Silva, R. C. D.; Ibrahim, S. A. Lactic acid bacteria: Food safety and human health applications. *Dairy* **2020**, *1* (3), 202–232.

(6) Bhat, B.; Bajaj, B. K. Multifarious cholesterol lowering potential of lactic acid bacteria equipped with desired probiotic functional attributes. *3 Biotech* **2020**, *10* (5), No. 200.

(7) Markiewicz-Kęszycka, M.; Czyżak-Runowska, G.; Lipińska, P.; Wójtowski, J. Fatty acid profile of milk—a review. *Bull. Vet. Inst. Pulawy* **2013**, *57*, 135–139.

(8) Tudisco, R.; Chiofalo, B.; Addi, L.; Lo Presti, V.; Rao, R.; Calabro, S.; Musco, N.; Grossi, M.; Cutrignelli, M. I.; Mastellone, V.; Lombardi, P.; Infascelli, F. Effect of hydrogenated palm oil dietary supplementation on milk yield and composition, fatty acids profile and Stearoyl-CoA desaturase expression in goat milk. *Small Ruminant Res.* **2015**, *132*, 72–78.

(9) Liavonchanka, A.; Rudolph, M. G.; Tittmann, K.; Hamberg, M.; Feussner, I. On the mechanism of a polyunsaturated fatty acid double bond isomerase from *Propionibacterium acnes*. *J. Biol. Chem.* **2009**, *284*, 8005–8012.

(10) Luo, X.; Zhang, L. W.; Li, H. B.; Zhang, S.; Jiao, Y. H.; Wang, S. M.; Xue, C. H.; Fan, R. B. Comparison of enzymatic activity of two linoleic acid isomerases expressed in *E. coli*. *Mol. Biol. Rep.* **2013**, *40*, 5913–5919.

(11) Liavonchanka, A.; Hornung, E.; Feussner, I.; Rudolph, M. G. Structure and mechanism of the *Propionibacterium acnes* polyunsaturated fatty acid isomerase. *Proc. Natl. Acad. Sci. U.S.A.* **2006**, *103* (8), 2576–2581.

(12) He, X. H.; Shang, J. L.; Li, F.; Liu, H. Yeast cell surface display of linoleic acid isomerase from *Propionibacterium acnes* and its application for the production of trans-10, cis-12 conjugated linoleic acid. *Biotechnol. Appl. Biochem.* **2015**, *62*, 1–8.

(13) Zhang, B. X.; Rong, C. C.; Chen, H. Q.; Song, Y. D.; Zhang, H.; Chen, W. De novo synthesis of trans-10, cis-12 conjugated linoleic acid in oleaginous yeast *Yarrowia lipolytica*. *Microb. Cell Fact.* **2012**, *11*, No. 51.

(14) Gul, I.; Bogale, T. F.; Deng, J.; Wang, L.; Feng, J.; Tang, L. A high-throughput screening assay for the directed evolution-guided discovery of halohydrin dehalogenase mutants for epoxide ring-opening reaction. *J. Biotechnol.* **2020**, *311*, 19–24.

(15) Zhou, P. P.; Xu, N. N.; Yang, Z. F.; Du, Y.; Yue, C. L.; Xu, N.; Ye, L. D. Directed evolution of the transcription factor Gal4 for development of an improved transcriptional regulation system in *Saccharomyces cerevisiae*. *Enzyme Microb. Technol.* **2020**, *142*, No. 109675.

(16) Druiteika, G.; Sadauskas, M.; Malunavicius, V.; Lastauskiene, E.; Taujenis, L.; Gegeckas, A.; Gudiukaite, R. Development of a new *Geobacillus* lipase variant GDlip43 via directed evolution leading to identification of new activity-regulating amino acids. *Int. J. Biol. Macromol.* **2020**, *151*, 1194–1204.

(17) Zhu, F. C.; He, B. F.; Gu, F. L.; Deng, H.; Chen, C. W.; Wang, W. Y.; Chen, N. F. Improvement in organic solvent resistance and activity of metalloprotease by directed evolution. *J. Biotechnol.* **2020**, *309*, 68–74.

(18) Goering, A. W.; McClure, R. A.; Doroghazi, J. R.; Albright, J. C.; Haverland, N. A.; Zhang, Y. B.; Ju, K. S.; Thomson, R. J.; Metcalf, W. W.; Kelleher, N. L. Metabologenomics: Correlation of Microbial Gene Clusters with Metabolites Drives Discovery of a Nonribosomal Peptide with an Unusual Amino Acid Monomer. *ACS Cent. Sci.* **2016**, *2* (2), 99–108.

(19) Bensimon, A.; Heck, A. J. R.; Aebersold, R. Mass spectrometry-based proteomics and network biology. *Annu. Rev. Biochem.* **2012**, *81*, 379–405.

(20) Raamsdonk, L. M.; Teusink, B.; Broadhurst, D.; Zhang, N.; Hayes, A.; Walsh, M. C.; Berden, J. A.; Brindle, K. M.; Kell, D. B.; Rowland, J. J.; Westerhoff, H. V.; van Dam, K.; Oliver, S. G. A

functional genomics strategy that uses metabolome data to reveal the phenotype of silent mutations. *Nat. Biotechnol.* **2001**, *19* (1), 45–50.

(21) Zhao, S.; Zhou, Q. X.; Liu, D. M.; Wu, H.; Li, L.; Xu, X. L. Proteomic Analysis of L-lactic Acid Produced by *Bacillus coagulans*. *Chin. J. Food* **2020**, *20*, 212–225.

(22) Wiśniewski, J. R.; Zougman, A.; Nagaraj, N.; Mann, M. Universal sample preparation method for proteome analysis. *Nat. Methods* **2009**, *6*, 359–362.

(23) Zhang, Y. H.; Zeng, T.; Chen, L.; Huang, T.; Cai, Y. D. Determining protein-protein functional associations by functional rules based on gene ontology and KEGG pathway. *Biochim. Biophys. Acta, Proteins Proteomics* **2021**, *1869*, No. 140621.

(24) Tang, T. S.; Xu, Y.; Wang, J. F.; Tan, X.; Zhao, X. N.; Zhou, P.; Kong, F. D.; Zhu, C. Q.; Lu, C. P.; Lin, H. X. Evaluation of the differences between biofilm and planktonic *Brucella abortus* via metabolomics and proteomics. *Funct. Integr. Genomics* **2021**, *21*, 421–433.

(25) Jiang, L.; Cai, J.; Wang, J.; Liang, S.; Xu, Z.; Yang, S. T. Phosphoenolpyruvate-dependent phosphorylation of sucrose by *Clostridium tyrobutyricum* ZJU 8235: evidence for the phosphotransferase transport system. *Bioresour. Technol.* **2010**, *101*, 304–309.

(26) Kermani, A. A.; Roy, R.; Gopalingam, C.; Kocurek, K. I.; Patel, T. R.; Alderwick, L. J.; Besra, G. S.; Fütterer, K. Crystal structure of the TreS: Pep2 complex, initiating  $\alpha$ -glucan synthesis in the GlgE pathway of mycobacteria. *J. Biol. Chem.* **2019**, *294*, 7348–7359.

(27) Hemmi, H.; Yamashita, S.; Nakayama, T.; Nishino, T. Novel sugar phosphotransferase system applicable to the efficient labeling of the compounds synthesized via the non-mevalonate pathway in *Escherichia coli*. *J. Biosci. Bioeng.* **2002**, *93*, 515–518.

(28) Schneider, E.; Hunke, S. ATP-binding-cassette (ABC) transport systems: functional and structural aspects of the ATP-hydrolyzing subunits/domains. *FEMS Microbiol. Rev.* **1998**, *22*, 1–20.

(29) Wang, J. C.; Zhang, W. Y.; Zhong, Z.; Wei, A. B.; Bao, Q. H.; Zhang, Y.; Sun, T. S.; Postnikoff, A.; Meng, H.; Zhang, H. P. Gene expression profile of probiotic *Lactobacillus casei* Zhang during the late stage of milk fermentation. *Food Control* **2012**, *25* (1), 321–327.

(30) Ramadan, A. M.; Hassanein, S. E. Over-representation of repeats in stress response genes a strategy to increase versatility under stressful conditions. *C. R. Biol.* **2014**, *337*, 683–690.

(31) Wang, W.; Jeffery, C. J. An analysis of surface proteomics results reveals novel candidates for intracellular/surface moonlighting proteins in bacteria. *Mol. Syst. Biol.* **2016**, *12*, 1420–1431.

(32) Copley, S. D. An evolutionary biochemist's perspective on promiscuity. *Trends Biochem. Sci.* **2015**, *40*, 72–78.

(33) Butorac, A.; Dodig, I.; Bacun-Druzina, V.; Tishbee, A.; Mrvcic, J.; Hock, K.; Diminic, J.; Cindric, M. The effect of starvation stress on *Lactobacillus brevis* L62 protein profile determined by de novo sequencing in positive and negative mass spectrometry ion mode. *Rapid Commun. Mass Spectrom.* **2013**, *27* (9), 1045–1054.

(34) Bove, C. G.; Angelis, M. D.; Gatti, M.; Calasso, M.; Neviani, E.; Gobbetti, M. Metabolic and proteomic adaptation of *Lactobacillus rhamnosus* strains during growth under cheese-like environmental conditions compared to de Man, Rogosa, and Sharpe medium. *J. Proteomics* **2012**, *12*, 3206–3218.

(35) Dickely, F.; Nilsson, D.; Hansen, E. B.; Johansen, E. Isolation of *Lactococcus lactis* nonsense suppressors and construction of a food-grade cloning vector. *Mol. Microbiol.* **1995**, *15*, 839–847.

(36) Perna, N. T.; Plunkett, G., 3rd; Burland, V.; Mau, B.; Glasner, J. D.; Rose, D. J.; Mayhew, G. F.; Evans, P. S.; Gregor, J.; Kirkpatrick, H. A.; Posfai, G.; Hackett, J.; Klink, S.; Boutin, A.; Shao, Y.; Miller, L.; Grotbeck, E. J.; Davis, N. W.; Lim, A.; Dimalanta, E. T.; Potamousis, K. D.; Apodaca, J.; Anantharaman, T. S.; Lin, J.; Yen, G.; Schwartz, D. C.; Welch, R. A.; Blattner, F. R. Genome sequence of enterohaemorrhagic *Escherichia coli* O157:H7. *Nature* **2001**, *409* (6819), 529–533.

(37) Agarwal, K. C.; Miech, R. P.; Parks, R. E. J. Guanylate kinases from human erythrocytes, hogbrain, and rat liver. *Methods Enzymol.* **1978**, *51*, 483–490.

- (38) Goulian, M.; Beck, W. S. Purification and properties of cobamide-dependent ribonucleotide reductase from *Lactobacillus leichmannii*. *J. Biol. Chem.* **1966**, *241*, 4233–4242.
- (39) Boehme, R. E. Phosphorylation of the antiviral precursor 9-(1, 3-dihydroxy-2-propoxymethyl) guanine monophosphate by guanylate kinase isozymes. *J. Biol. Chem.* **1984**, *259*, 12346–12349.
- (40) Müller, C. W.; Schulz, G. E. Structure of the complex between adenylate kinase from *Escherichia coli* and the inhibitor Ap5A refined at 1.9Å resolution: A model for a catalytic transition state. *J. Mol. Biol.* **1992**, *224*, 159–177.